reversible Ru(VI)/Ru(IV) couple in acidic solutions as well as reversible Ru(VI)/Ru(V) and Ru(V)/Ru(IV) couples in basic solutions. Thus accurate redox potentials for these couples can be obtained. Second, the stability and rigidity imposed by the TMC ligand ensures that the complex and its reduced products persist in solution, thus giving rise to clean behavior. These factors together account for the detailed kinetics, thermodynamic, and mechanistic information that can be obtained in this study. Such information, apart from improving our understanding of high-valent ruthenium–oxo chemistry, would also help in the designing of efficient and selective ruthenium oxidants.

Electrochemical studies on other *trans*-dioxoruthenium(VI) species such as *trans*-$[Ru^{VI}(bpy)_2O_2]^{2+}$,[2e] indicated that their behavior is very similar to that of *trans*-$[Ru^{VI}(TMC)O_2]^{2+}$. It seems that the disproportionation mechanism that we established in this study is a general one for the *trans*-dioxoruthenium(V) species. Moreover, this work implies that other d^3 metal–oxo systems should also be unstable, and disproportionation of an oxo–manganese(IV) porphyrin system has been postulated recently.[24]

The observed large self-exchange rates of the Ru(VI)/(V) and Ru(V)/(IV) couples and rate of disproportionation of Ru(V) suggest that the redox interconversion between Ru(VI) and Ru(IV) is rapid. This explains the reversibility of the two-electron Ru(VI)/(IV) couple observed in the electrochemistry of *trans*-dioxoruthenium(VI).

Acknowledgment. We thank the Croucher Foundation, the University and Polytechnic Granting Committee, and the University of Hong Kong for financial support.

Registry No. *trans*-$[Ru^{VI}(TMC)(O)_2]^{2+}$, 95978-17-9; $[Ru^{II}(NH_3)_4bpy]^{2+}$, 54194-87-5; $[Ru^{II}(NH_3)_5isn]^{2+}$, 19471-53-5; $[Ru^{II}(NH_3)_5py]^{2+}$, 21360-09-8; *trans*-$[Ru^{V}(TMC)(O)_2]^{+}$, 103056-17-3.

Supplementary Material Available: Figure S1 of the spectrophotometric titration of *trans*-$[Ru^{VI}(TMC)(O)_2]^{2+}$ with *cis*-$[Ru^{II}(NH_3)_4bpy]^{2+}$ at 522 nm (1 page). Ordering information is given on any current masthead page.

(24) Groves, J. T.; Stern, M. K. *J. Am. Chem. Soc.* **1987**, *109*, 3812.

Polynuclear ((Diphenylphosphino)methyl)phenylarsine Bridged Complexes of Gold(I). Bent Chains of Gold(I) and a Role for Au(I)–Au(I) Interactions in Guiding a Reaction

Alan L. Balch,* Ella Y. Fung, and Marilyn M. Olmstead

Contribution from the Department of Chemistry, University of California, Davis, California 95616. *Received February 5, 1990*

Abstract: The role of weak Au(I)–Au(I) interactions in determining the structure and reactivity of a set of new, ligand-bridged complexes is described. Addition of 2 equivs of Me_2SAuCl to dpma [dpma is bis((diphenylphosphino)methyl)phenylarsine] yields $Au_2Cl_2(\mu$-dpma) which has its two gold ions widely separated (7.011 (1) Å) but which packs about a center of symmetry so that there are two close (3.141 (1) Å) Au–Au contacts between molecules. ^{31}P NMR spectra indicate that this molecule self associates at low temperature in solution also. Treatment of $Au_2Cl_2(\mu$-dpma) with further Me_2SAuCl produces $Au_3Cl_3(\mu$-dpma) which has a bent Au_3 chain (Au–Au distances 3.131 (1), 3.138 (1) Å; Au–Au–Au angle, 110.9 (1)°). The reaction of $Au_2Cl_2(\mu$-dpma) with ammonium hexafluorophosphate or thallium nitrate yields $[Au_4Cl_2(\mu\text{-dpma})_2][PF_6]_2$ or $[Au_4Cl_2(\mu\text{-dpma})_2][NO_3]_2$, respectively. These have bent Au_4 chains (Au–Au distances 2.965 (1), 3.096 (1); Au–Au–Au angle, 88.0 (1)° in the hexafluorophosphate salt) with terminal P–Au–Cl groups and the dpma ligands aligned so that phosphorus is trans to arsenic on the central two gold ions. Comparisons of the solid state, associated form of $Au_2Cl_2(\mu$-dpma) and $[Au_4Cl_2(\mu\text{-dpma})_2]^{2+}$ suggest that the initial stage of formation of the Au_4 chain involves association of the $Au_2Cl_2(\mu$-dpma) units through Au–Au interactions, despite the presence of vacant coordination sites on the gold ions and lone pairs on the arsenic atoms. The role of empty p acceptor orbitals on gold favoring the bent chains is developed.

Recent work on molecular recognition has focused attention on bonding interactions between molecules which are generally weaker than normal covalent bonds.[1] Among those are hydrogen bonds, electron donor/acceptor interactons and van der Waal's forces. The attractive interaction between Au(I) centers is another such interaction which, while weak, has important effects in determining molecular conformations and packing within gold(I) complexes.[2] It has been suggested[3] that Au/Au contacts shorter than 3.5 Å are otherwise unexpected for such a large ion and it has been known that short Au–Au contacts (as short as 2.776 Å)[4] are frequently seen in the solid state.[3] Only recently, however, has it been possible to estimate the energy associated with such bonds. Schmidbaur and co-workers have estimated that a Au–Au interaction (with a bond distance of 3.000 Å) has a bond energy of 7–8 kcal mol^{-1}.[5]

Most of the observed Au–Au interactons in Au(I) compounds involve pairs of gold ions,[6] but a few examples of extended Au–Au interactions involving three or more gold ions are known.[4] Here we present new structural data that show the ability of Au–Au interactions to orient molecules in the solid state in a configuration which is suggestive of an intermediate that is suitable for a reaction observed in solution. These interactions result in the formation of bent groups of three or four gold(I) ions. For this we used a flexible ligand, bis((diphenylphosphino)methyl)phenylarsine (dpma), that places minimal constraints on the gold–gold separations. Previous work with this ligand has focused on the use

(1) Lehn, J.-M. *Angew. Chem., Int. Ed. Engl.* **1988**, *27*, 89. Cram, D. J. *Angew. Chem., Int. Ed. Engl.* **1986**, *25*, 1039. *Host Guest Chemistry*; Parts I–III, Vögtle, F., Weber, E., Eds.; *Top Curr.* **1984**, **1982**, **1981**, *121*, *101*, *98*.

(2) Schmidbaur, H. *Angew. Chem., Int. Ed. Engl.* **1976**, *15*, 728. Schmidbaur, H.; Dash, K. C. *Adv. Inorg. Chem. Radiochem.* **1982**, *25*, 239. Puddephatt, R. J. *The Chemistry of Gold*; Elsevier: Amsterdam, 1978.

(3) Jones, P. G. *Gold Bull.* **1981**, *14*, 102; **1981**, *14*, 159; **1983**, *16*, 114; **1986**, *19*, 46.

(4) Inoguchi, Y.; Milewski-Mahrla, B.; Schmidbaur, H. *Chem. Ber.* **1982**, *115*, 3085.

(5) Schmidbaur, H.; Graf, W.; Müller, G. *Angew. Chem., Int. Ed. Engl.* **1988**, *27*, 417.

(6) Throughout, our discussion is restricted to d^{10} Au(I) species, and we specifically exclude more reduced gold clusters from consideration. For emphasis, structural drawings use solid lines for the gold–gold interactions.

0002-7863/90/1512-5181$02.50/0

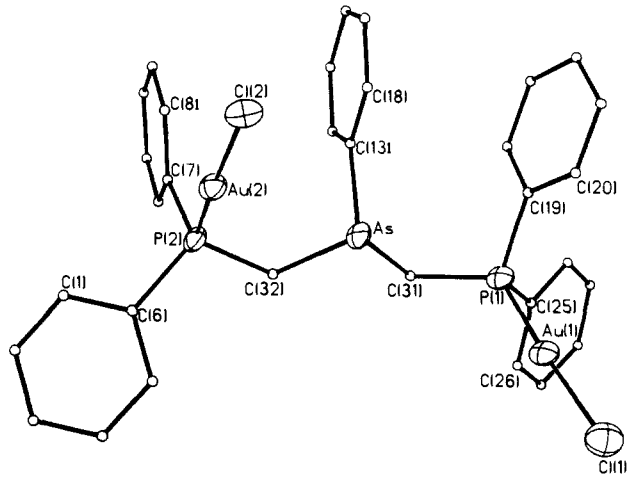

Figure 1. A perspective view of $Au_2Cl_2(\mu$-dpma) with 50% thermal contours for the heavy atoms and uniform, arbitrarily sized circles for carbon atoms. Interatomic distances (Å): Au(1)···Au(2), 7.011; Au–P(1), 2.239 (4); Au(2)–P(2), 2.233 (4); Au(1)–Cl(1), 2.289 (4); Au(2)–Cl(2), 2.298 (4). Interatomic angles (deg): P(1)–Au(1)–Cl(1), 172.5 (2); P(2)–Au(2)–Cl(2), 172.5 (1).

of the metallomacrocycle, **1**, to form trinuclear complexes, **2**, by addition of a third metal ion to the central cavity of **1** (eq 1).[7] While a gold(I)-containing analogue of **1** would be a useful material for the preparation of other trinuclear complexes, this type of open metallomacrocycle does not form in the reactions described here.

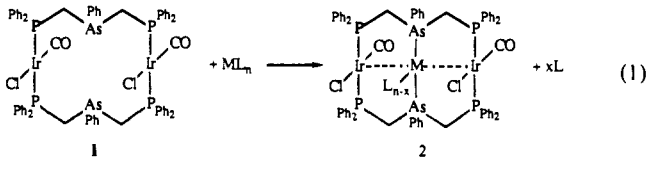

Results

$Au_2Cl_2(\mu$-dpma). Treatment of dpma in toluene solution with 2 equivs of (dimethyl sulfide)gold(I) chloride in dichloromethane yields a colorless solution from which colorless crystals of $Au_2Cl_2(\mu$-dpma) are obtained in 86% yield after the addition of diethyl ether (eq 2). In dichloromethane solution these give a singlet in the $^{31}P\{^1H\}$ NMR spectrum at 23.9 ppm. (Free dpma gives a singlet at −20.9 ppm.)

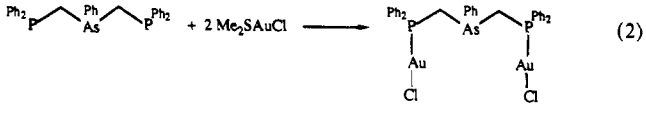

The complex crystallizes with one molecule of $Au_2Cl_2(\mu$-dpma) and 2.5 molecules of toluene in the asymmetric unit. A drawing of the molecule is shown in Figure 1, and some significant molecular dimensions are given in the figure caption. As expected,[8] gold(I) binds preferentially to the phosphorus atoms of dpma, and the arsenic atom is left uncoordinated. The P–Au–Cl units are nearly linear. Within the molecule the two P–Au–Cl units are widely spaced. The distance between the two gold ions is 7.011 (1) Å.

Although within a single molecule there is not significant Au···Au contact, there are interesting interactions between two adjacent molecules. This is best appreciated by turning to the stereoscopic drawing presented in Figure 2. This shows the arrangement of a pair of molecules of $Au_2Cl_2(\mu$-dpma) that pack about a center of symmetry in the solid. Two close Au–Au

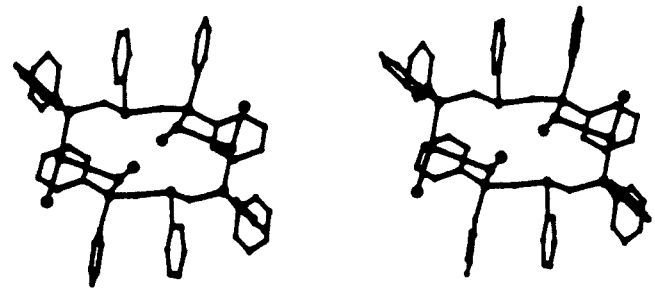

Figure 2. A stereoscopic view showing the interaction between two molecules of $Au_2Cl_2(\mu$-dpma) in the crystal. The short gold–gold contacts are shown as solid lines.

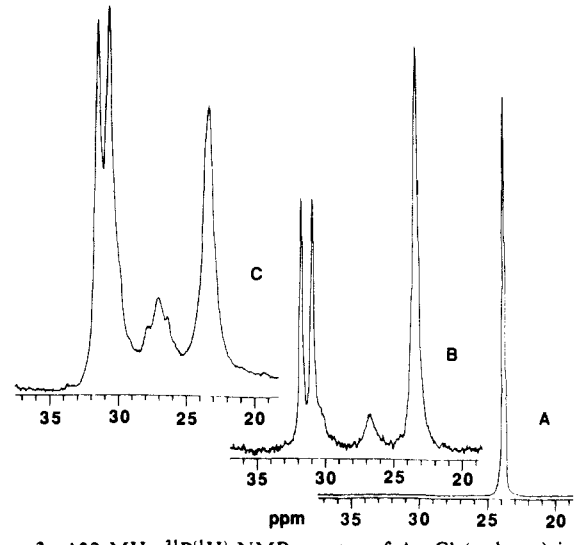

Figure 3. 122 MHz $^{31}P\{^1H\}$ NMR spectra of $Au_2Cl_2(\mu$-dpma) in dichloromethane (A) 0.307 M at 23 °C, (B) 0.0192 M at −80 °C, and (C) 0.0769 M at −80 °C.

contacts occur between the two molecules. Since the pair is centrosymmetric, both of these are identical with a short Au–Au separation of 3.141 (1) Å. These are the shortest contacts within this molecular pair. For example, the Cl···Cl separation is much larger (4.753 (6) Å). The As···Au contact (3.393 (1) Å) is too long for bonding. Moreover, the lone pair on arsenic points 47° away from the As–Au vector. The phenyl ring, C(1)–C(6), on P(1) lies so that it faces one of the gold atoms of the other molecule within the pair. However, the Au–C distances are relatively long again ranging from 3.895 Å for Au(1) to C(1′) to 5.175 Å for Au(1) to C(4′)).

In order to detect association in solution, the $^{31}P\{^1H\}$ NMR spectrum of $Au_2Cl_2(\mu$-dpma) in dichloromethane was obtained under a variety of conditions. At 23 °C under all concentrations examined (up to 0.3 M), the spectrum consisted of a single line at 23.9 ppm. The spectrum of an 0.309 M solution is shown as trace A of Figure 3. On cooling, however, the spectrum broadens and additional lines are seen. Trace B of Figure 3 shows the spectrum of a 0.0192 M solution at −80 °C. Two new resonances, 31.8 and 30.9 ppm, are present along with a shoulder to high field and a broad line at 27.0 ppm. On increasng the concentration to 0.0769 M as shown in trace C, the intensity of the doublet grows at the expense of the singlet at 23.4 ppm. The resonance at 27.0 ppm also grows and gains some structure, and all lines broaden. The new resonances are assigned to aggregated species since their intensities grow with increasing concentration. The doublet at 31.8 and 30.9 ppm is likely to be due to a centrosymmetric dimer analogous to that seen in the solid state.

$Au_3Cl_3(\mu$-dpma). Addition of 3 equivs of (dimethyl sulfide)gold(I) chloride to dpma or 1 equiv of (dimethyl sulfide)gold(I) chloride to $Au_2Cl_2(\mu$-dpma) in dichloromethane leads to the spontaneous precipitation of colorless crystals of $Au_3Cl_3(\mu$-dpma) (eq 3). These have negligible solubility in nondonor solvents (dichloromethane, chloroform, benzene, and toluene), and for that

(7) For examples, see: Balch, A. L. *Pure Appl. Chem.* **1988**, *60*, 555. Balch, A. L.; Olmstead, M. M.; Oram, D. E.; Reedy, P. E., Jr.; Reimer, S. H. *J. Am. Chem. Soc.* **1989**, *111*, 4021 and references in each.

(8) Ahrland, S.; Chatt, J.; Davies, N. R. *Quart. Rev., Chem. Soc.* **1958**, *12*, 265. Balch, A. L.; Fossett, H. L. A.; Olmstead, M. M.; Reedy, P. E., Jr. *Organometallics* **1986**, *5*, 1929.

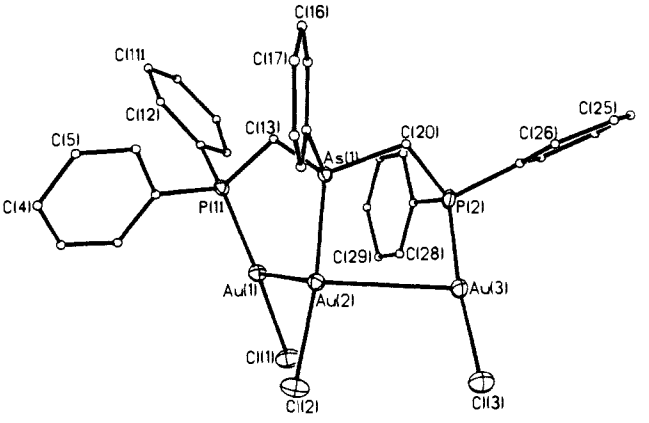

Figure 4. A perspective view of $Au_3Cl_3(\mu$-dpma) with 50% thermal contours for the heavy atoms and uniform, arbitrarily sized circles for carbon atoms. Interatomic distances (Å): Au(1)–Au(2), 3.131 (1); Au(2)–Au(3), 3.138 (1); Au(1)···Au(3), 5.163 (1); Au(1)–P(1), 2.234 (4); Au(3)–P(2), 2.227 (4); Au(2)–As, 2.336 (1); Au(1)–Cl(1), 2.303 (4); Au(2)–Cl(2), 2.288 (4); Au(3)–Cl(3), 2.278 (4). Interatomic angles (deg): P(1)–Au(1)–Cl(1), 175.5 (2); As–Au(2)–Cl(2), 172.2 (1); P(2)–Au(3)–Cl(3), 173.3 (2); Au(1)–Au(2)–Au(3), 110.9 (1).

reason it has not been possible to obtain a ^{31}P NMR spectrum for this material.

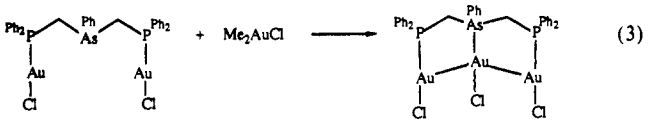

The structure of the complex as determined by X-ray crystallography is shown in Figure 4 with interatomic distances and angles given in the caption. The substance crystallized with one molecule of the complex and one of dichloromethane in the asymmetric unit. The introduction of the third gold ion has caused the $Au_2Cl_2(\mu$-dpma) skeleton to contract about this unit. There are now two short intramolecular Au–Au contacts (3.131 (1) and 3.138 (1) Å). Moreover, the nonbonded Au(1)···Au(3) separation is reduced to 5.163, whereas it was 7.011 Å in $Au_2Cl_2(\mu$-dpma). The P–Au–Cl and As–Au–Cl units are nearly linear. The Au(1)–Au(2)–Au(3) angle is 110.9°. There are no significant intermolecular contacts in this solid.

$[Au_4Cl_2(\mu$-dpma)$_2][PF_6]_2$ and $[Au_4Cl_2(\mu$-dpma)$_2][NO_3]_2$. In polar solvents, $Au_2Cl_2(\mu$-dpma) readily looses a chloride ion and is converted into a tetranuclear complex as shown in eq 4. Thus,

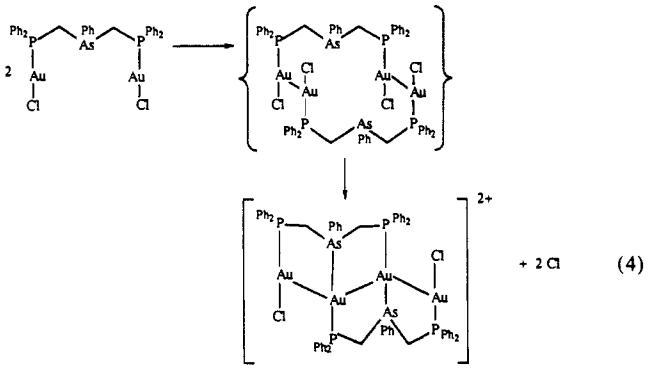

treatment of a dichloromethane solution of $Au_2Cl_2(\mu$-dpma) with a methanolic solution of ammonium hexafluorophosphate results in the precipitation of colorless crystals of $[Au_4Cl_2(\mu$-dpma$)_2][PF_6]_2$. The tetraphenylborate salt is obtained similarly with the use of sodium tetraphenylborate. The nitrate salt, $[Au_4Cl_2(\mu$-dpma$)_2][NO_3]_2$, and thallium chloride form when a dichloromethane solution of $Au_2Cl_2(\mu$-dpma) is treated with thallium nitrate in a methanol/dichloromethane mixture. The structures of both the hexafluorophosphate and the nitrate salt have been determined by X-ray crystallography. The cations in each are similar. Figure 5 shows the entire structure of the cation that occurs in the hexafluorophosphate salt. Figure 6 shows another view of the inner coordination region with the phenyl groups omitted. Table I allows comparison of selected bond distances and angles for the cations in the two different salts.

Table I. Selected Interatomic Distances and Angles in $[Au_4Cl_2(\mu$-dpma$)_2]^{2+}$

	$[Au_4Cl_2(\mu$-dpma$)_2][PF_6]_2\cdot 2CH_2Cl_2\cdot 2H_2O$	$[Au_4Cl_2(\mu$-dpma$)_2][NO_3]_2\cdot 4CH_3OH$
	Distances (Å)	
Au(2)–Au(2′)	2.965 (1)	3.014 (2)
Au(1)–Au(2)	3.096 (1)	3.110 (2)
Au(1)···Au(2′)	4.212 (1)	4.023 (2)
Au(1)–P(1)	2.236 (4)	2.236 (7)
Au(1)–Cl	2.298 (4)	2.300 (6)
Au(2)–As	2.419 (2)	2.425 (3)
Au(2)–P(2)	2.302 (4)	2.306 (6)
P(1)···As	3.109 (6)	3.113 (8)
P(2′)···As	3.128 (6)	3.158 (8)
	Angles (deg)	
Au(1)···Au(2)···Au(2′)	88.0 (1)	82.1 (2)
As–Au(2)–P(2)	170.3 (1)	172.7 (2)
Cl–Au(1)–P(1)	176.5 (2)	176.4 (2)

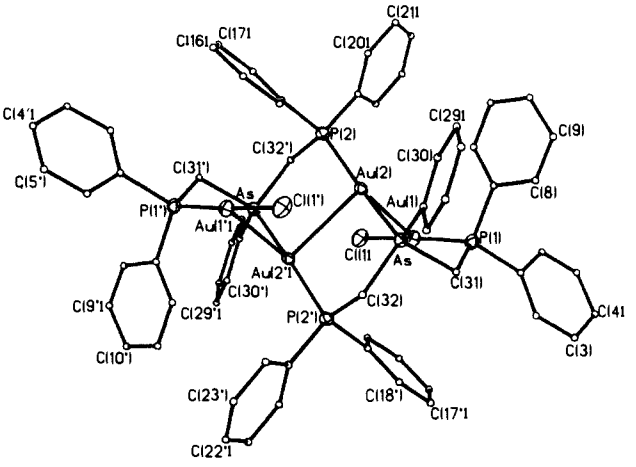

Figure 5. A perspective view of the cation in $[Au_4Cl_2(\mu$-dpma$)_2][PF_6]_2$ with 50% thermal contours for the heavy atoms and uniform, arbitrarily sized circles for carbon atoms.

In both salts the cation is centrosymmetric with a folded Au_4 chain. The Au(1)–Au(1′)–Au(2) angle is 88.0 (1)° in the hexafluorophosphate structure. The two bridging dpma ligands are arranged so that phosphorus is trans to arsenic on Au(2) and Au(2′). This alignment of the dpma ligands contrasts with that seen in the metallomacrocycle **1** and its adducts. However, a related arrangement of the bridging ligands is seen in the nearly linear, tetranuclear complex, $Rh_4(\mu$-CO)(CO)$_2(\mu$-Cl)$_2(\mu$-$(Ph_2P)_2$py), where $(Ph_2P)_2$py is 2,6-bis(diphenylphosphino)-pyridine.[9] Within the cation, each gold has linear coordination to two donor atoms and additional short contacts with other gold centers. The central Au(2)–Au(2′) distance (2.965 (1) Å) is shorter than the external Au(1)–Au(2) separation (3.096 (1)°). In both cases these gold–gold contacts are shorter than the nonbonding P···As separations on the dpma ligands. This has been used as a criterion of the existence of metal–metal bonding.

Discussion

Gold–gold interactions play a prominent role in all three structural types of gold(I) complexes here. Comparison of the structures of the dimeric $\{Au_2Cl_2(\mu$-dpma$)_2\}_2$ unit shown in Figure 2 and the cation $[Au_4Cl_2(\mu$-dpma$)_2]^{2+}$ shown in Figure 5 reveals that these molecules are closely related. In the neutral dimer, the significant contacts are the two Au–Au interactions. Note in particular that Au–Au not Au–As interactions are found in the structure of this novel dimer. These Au–Au interactions occur despite the fact that the arsenic lone pairs are fully available to bind to the coordinatively unsaturated 14-electron gold(I) com-

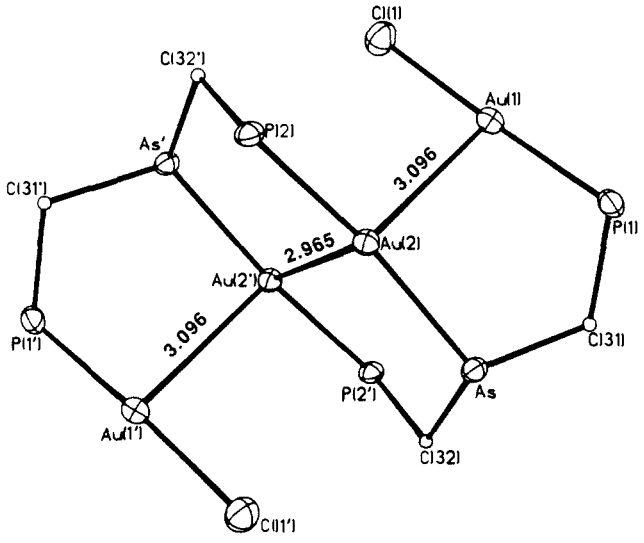

Figure 6. A view of the inner coordination of the cation in $[Au_4Cl_2(\mu\text{-dpma})_2][PF_6]_2$ with the phenyl groups omitted.

plexes. Upon viewing Figure 2 the reader will see that the structure of $Au_2Cl_2(\mu\text{-dpma})$ in the solid state appears well on its way toward conversion into the tetragold dication. Conversion of this unit into the tetragold dication would require three major changes: coordination of the two arsenic atoms to the adjacent gold atoms (the Au···As distance involved is 3.393 Å), loss of the two chloride ligands on the affected gold centers through ionization, and movement of these two gold ions together (their separation is 4.904 Å in $\{Au_2Cl_2(\mu\text{-dpma})\}_2$). The ^{31}P NMR data in Figure 3 indicate that aggregation of $Au_2Cl_2(\mu\text{-dpma})$ can occur at significant concentrations in solution particularly at low temperatures, where the entropic contribution to dissociation is lessened. We suggest that this aggregation occurs through Au–Au interactions like those seen in Figure 2 and that the initial step in the formation of $[Au_4Cl_2(\mu\text{-dpma})_2]^{2+}$ involves association of $Au_2Cl_2(\mu\text{-dpma})_2$ through Au–Au bonding corresponding to what is seen in the solid state (Figure 2). This appears to be the first case in which these weak Au–Au interactions can be assigned a role in guiding the course of a chemical reaction. The ability to detect association between molecules of $Au_2Cl_2(\mu\text{-dpma})_2$ in solution is no doubt enhanced by the fact that two Au–Au interactions occur between pairs of molecules. In designing other molecules to explore the nature of weak interactions like those between Au(I) ions, it may be useful to incorporate several such sites within a molecule in order to take advantage of enhanced bonding between polyfunctional molecules.

The Au_3 and Au_4 chains in $Au_3Cl_3(\mu\text{-dpma})$ and $[Au_4Cl_2(\mu\text{-dpma})_2]^{2+}$ are decidedly bent. These can be compared to complexes containing a variety of extended Au–Au interactions. A number of dimeric gold(I) complexes form nearly linear extended chains. An example is $[\{(i\text{-Pr})_2PS_2\}_2Au_2]_n$ with intramolecular gold–gold separations at 2.914 (5) and 3.097 (6) Å, intermolecular separations of 3.050 (6) and 3.109 (6) Å, and Au–Au–Au angles ranging from 176.6 (2) to 178.9 (2)°.[10] A qualitative molecular orbital analysis of binuclear Au(I) complexes and their polymers indicates that the Au–Au bonding interaction arises from mixing of the filled d_{z^2} orbitals and the empty s and p_z orbitals (where the z axis lies along the Au–Au bond).[11] These calculations also show how this can be extended along the z direction. Aggregates formed by associations of monomeric Au(I) complexes take on a wide variety of structures that range from nearly linear extended chains (as found in Me_2SAuCl with an Au–Au distance of 3.226 (1) Å and an Au–Au–Au angle of 168.1°)[12] to a nearly square arrangement of four Au(I) centers (as found in (piperidine)AuCl where the Au–Au distance is 3.301 (5) Å and the Au–Au–Au angle is 88.3 (1)°).[13] This latter example, along with the dpma-bridged complexes described here, demonstrates that the Au–Au–Au unit is flexible and is not limited to linear chains. Additionally, $Au_3Cl_3(\mu\text{-dpma})$ may be compared to $[Au_3Cl_2(\mu\text{-dpm})_2]^+$ where the Au–Au distances are 3.164 (5) and 3.067 (5) Å and the chain is sharply bent so that the Au–Au–Au angle is 72.3°.[14] In these phosphine-bridged aggregates, the ligand

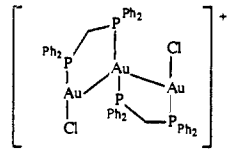

backbone itself cannot be solely responsible for the bending of the chains. There is no ligand constraint on the Au–Au–Au angle in the case of $[Au_3Cl_2(\mu\text{-dpm})_2]^+$, and it is known that complexes with *two* dpma bridges (where any effect of the ligand bridge would be increased) can be much more nearly linear than observed for either the Au_3 or Au_4 chains described here.[7,15] We suspect that the bending of the Au–Au–Au units seen here arises from an electronic effect that results from the incorporation of both empty p orbitals on the bent gold in the Au–Au bonding. Bending of the chain then allows additional acceptor orbitals to be incorporated into the bonding of these chains and results in some net stabilization. Since these Au–Au interactions are, however, intrinsically weak, the added stability gained by bending of a Au_n unit will not always be sufficient to determine its structure.

$Au_2Cl_2(\mu\text{-dpma})$ with its uncoordinated arsenic atom may be considered as a metalloligand that is useful as a building block for the construction of other polynuclear complexes. A simple example involves its reaction with Me_2SAuCl to form $Au_3Cl_3(\mu\text{-dpma})$. Other examples of reactions utilizing $Au_2Cl_2(\mu\text{-dpma})$ as a ligand are described in a separate article.[16] Notice that the formation of $Au_3Cl_3(\mu\text{-dpma})$ brings all three gold atoms together within the complex itself. This contrasts with the behavior of other AuCl complexes of polyphosphine ligands where the Au/Au interactons are limited to pairs of Au(I) centers that can occur in a variety of different ways. Simple, short intramolecular Au–Au contacts are seen in $Au_2Cl_2(\mu\text{-dpm})$,[17] $Au_2Cl_2\{\mu\text{-}(Ph_2P)_2C{=}PMe_3\}$,[5] and $Au_2Cl_2(\mu\text{-}cis\text{-}Ph_2PCHCHPPh_2)$.[18] In $Au_2Cl_2(\mu\text{-}Ph_2P(CH_2)_3PPh_2)$, however, the intramolecular Au/Au separation is quite long, but there are close (<3.17 Å) Au–Au contacts between molecules that produce a polymeric chain structure in the solid.[19] In $Au_3Cl_3(\mu\text{-}(Ph_2PCH_2)_3CMe)$ two of the gold centers are separated by only 3.091 Å, while the third gold center is located at a much more remote site.[20] $Au_2Cl_2(\mu\text{-}Ph_2P(CH_2)_2PPh_2)$ has a structure resembling that of $Au_2Cl_2(\mu\text{-dpma})$ in which the intermolecular Au···Au separation is long, but the molecules pack about a center of symmetry so that there are two close Au–Au contacts within each molecular pair.[21]

Experimental Section

Preparation of Compounds. (Dimethyl sulfide)gold(I) chloride[2] and dpma were prepared by established routes.[23]

$Au_2Cl_2(\mu\text{-dpma})$. A solution of 535 mg (1.82 mmol) of Me_2SAuCl

(9) Wood, F. E.; Olmstead, M. M.; Balch, A. L. *J. Am. Chem. Soc.* **1983**, *105*, 6332.
(10) Lawton, S. L.; Rohrbaugh, W. J.; Kokotailo, G. T. *Inorg. Chem.* **1972**, *11*, 2227.
(11) Jiang, Y.; Alvarez, S.; Hoffmann, R. *Inorg. Chem.* **1985**, *24*, 749.
(12) Jones, P. G.; Lautner, J. *Acta Crystallogr.* **1988**, *C44*, 2089.
(13) Guy, J. J.; Jones, P. G.; Mays, M. J.; Sheldrick, G. M. *J. Chem. Soc., Dalton Trans.* **1977**, 8.
(14) Usõn, R.; Laguna, A.; Laguna, M.; Fernandez, E.; Villacampa, M. D.; Jones, P. G.; Sheldrick, G. M. *J. Chem. Soc., Dalton Trans.* **1983**, 1679.
(15) Balch, A. L.; Nagle, J. K.; Oram, D. E.; Reedy, P. E., Jr. *J. Am. Chem. Soc.* **1988**, *110*, 454.
(16) Balch, A. L.; Fung, E. Y.; Olmstead, M. M. *Inorg. Chem.* In press.
(17) Schmidbaur, H.; Wohlleben, A.; Wagner, F.; Orama, O.; Huttner, G. *Chem. Ber.* **1977**, *110*, 1748.
(18) Jones, P. G. *Acta Crystallogr.* **1980**, *B36*, 2775.
(19) Cooper, M. K.; Mitchell, L. E.; Henrick, K.; McPartlin, M.; Scott, A. *Inorg. Chim. Acta* **1984**, *84*, 69.
(20) Cooper, M. K.; Henrick, K.; McPartlin, M.; Latten, J. L. *Inorg. Chim. Acta* **1982**, *65*, L185.
(21) Bartes, P. A.; Waters, J. M. *Inorg. Chim. Acta* **1985**, *98*, 125.
(22) Ray, p. C.; Sen, S. C. *J. Indian Chem. Soc.* **1930**, *7*, 67.
(23) Balch, A. L.; Fossett, L. A.; Olmstead, M. M.; Oram, D. E.; Reedy, P. E., Jr. *J. Am. Chem. Soc.* **1985**, *107*, 5272.

Table II. Crystal Data and Data Collection Parameters for Complexes

	$Au_2Cl_2(\mu$-dpma)	$Au_3Cl_3(\mu$-dpma)	$[Au_4Cl_2(\mu$-dpma$)_2](PF_6)_2$	$[Au_4Cl_2(\mu$-dpma$)_2](NO_3)_2$
formula	$C_{46}H_{45.5}AsAu_2Cl_2P_2$	$C_{33}H_{31}AsAu_3Cl_5P_2$	$C_{66}H_{58}As_2Au_4Cl_6F_{12}O_2P_6$	$C_{68}H_{70}As_2Au_4Cl_2N_2O_{10}P_4$
fw	1200.08	1332.65	2447.45	2207.82
color and habit	colorless blocks	colorless needles	colorless prisms	colorless prisms
crystal system	triclinic	monoclinic	monoclinic	monoclinic
space group	$P\bar{1}$	$P2_1/n$	$P2_1/n$	$C2/c$
a, Å	13.687 (3)	15.515 (3)	12.403 (3)	19.869 (3)
b, Å	14.436 (4)	16.931 (3)	19.154 (5)	14.387 (2)
c, Å	14.465 (3)	16.117 (3)	16.267 (9)	24.915 (2)
α, deg	111.66 (2)			
β, deg	97.03 (2)	117.72 (1)	90.33 (3)	91.70 (2)
γ, deg	113.62 (2)			
V, Å^3	2308 (1)	3747 (1)	3864 (2)	7120 (2)
T, K	130	130	130	130
Z	2	4	2	4
cryst dimens, mm	0.30 × 0.30 × 0.45	0.10 × 0.12 × 0.43	0.15 × 0.13 × 0.23	0.13 × 0.25 × 0.30
d_{calcd}, g cm^{-3}	1.73	2.36	2.10	1.92
radiation, (Å)	Mo Kα, (λ = 0.71069)			
μ (Mo Kα), cm^{-1}	72.62	130.4	88.06	93.43
range of transm factors	0.09–0.18	0.20–0.34	0.25–0.40	0.16–0.37
diffractometer	$P2_1$, graphite monochromator			
scan method	ω	ω	ω	ω
scan range, degrees	1.5	1.0	1.1	1.4
offset for bkgnd, degrees	1.2	1.0	1.1	1.0
scan speed, deg min^{-1}	15	8	15	15
2θ range, deg	0–50	0–50	0–50	0–50
octants collected	$h,\pm k,\pm l$	$h,k,\pm l$	$h,k,\pm l$	$h,k,\pm l$
no. data collected	7905	7009	7441	6804
no. unique data	7905	6511 [R(merge) = 0.006]	7205 [R(merge) = 0.013]	6528 [R(merge) = 0.023]
no. data used in refinement	5629 [$I > 3\sigma(I)$]	4079 [$I > 2\sigma(I)$]	3866 [$I > 3\sigma(I)$]	3626 [$I > 3\sigma(I)$]
no. parameters refined	177	232	274	215
R[a]	0.065	0.051	0.049	0.088
R_w[a]	0.071 [$w = 1/\sigma^2(F_o)$]	0.057 [$w = 1/\sigma^2(F_o)$]	0.048 [$w = 1/\sigma^2(F_o)$]	0.091 [$w = 1/\sigma^2(F_o)$]

[a] $R = \sum||F_o| - |F_c||/|F_o|$ and $R_w = \sum||F_o| - |F_c||w^{1/2}\sum|F_o w^{1/2}|$.

in a minimum volume of dichloromethane was added to a solution of 500 mg (0.908 mmol) of dpma in a minimum volume of toluene. The solution was filtered, and after 30 min ethyl ether was added dropwise. The white precipitate was collected by filtration and washed with ethyl ether. The product may be recrystallized by dissolution in dichloromethane and precipitation by the addition of ethyl ether; yield, 793 mg (86%).

$Au_3Cl_3(\mu$-dpma). Method 1. A filtered solution of 150 mg (0.509 mmol) of Me_2SAuCl in a minimum volume of dichloromethane was added to a filtered solution of 93.4 mg (0.170 mmol) of dpma in a minimum volume of dichloromethane. The white, crystalline product formed rapidly. It was collected by filtration and washed in the dichloromethane and ethyl ether: yield, 196 mg (93%).

Method 2. A filtered solution of 9.5 mg (0.0323 mmol) of Me_2SAuCl in a minimum volume of dichloromethane was added to a filtered solution of 32.8 mg (0.0323 mmol) of $Au_2Cl_2(\mu$-dpma) in a minimum volume of dichloromethane. The white crystalline solid that precipitated was collected by filtration, washed with dicloromethane and ethyl ether, and vacuum dried: yield, 28.1 mg (70%).

$[Au_4Cl_2(\mu$-dpma$)_2][PF_6]_2$. A filtered solution of 37.0 mg (0.227 mmol) of ammonium hexafluorophosphate in a minimum volume of 1:1 methanol/dichloromethane was added dropwise to a stirred, filtered solution of 59.2 mg (0.0583 mmol) of $Au_2Cl_2(\mu$-dpma) in a minimum volume of dichloromethane. The white, crystalline solid that formed was collected by filtration, washed with methanol and dried under vacuum: yield, 50.2 mg (77%).

$[Au_4Cl_2(\mu$-dpma$)_2][NO_3]_2$. A solution of 6.1 mg (0.02 mmol) of thallium nitrate in a minimum volume 2:1 of methanol/dichloromethane was added dropwise to a solution of $Au_2Cl_2(\mu$-dpma) in minimum volume of dichloromethane. The solution was filtered to remove solid thallium chloride. On evaporation, crystals of the product slowly formed.

Because of the limited solubility of these salts in noncoordinating solvents, it has not been possible to obtain their ^{31}P NMR spectra.

X-ray Data Collection. $Au_2Cl_2(\mu$-dpma$)\cdot 2.5C_6H_5CH_3$. Colorless blocks were formed by slow diffusion of diethyl ether into dichloromethane solution of $Au_2Cl_2(\mu$-dpma$)\cdot 2.5C_7H_8$. The crystals were removed from the diffusion tube and rapidly coated with a light hydrocarbon oil to reduce the loss of solvent from the crystal. The crystal was mounted in the cold stream of a Syntex $P2_1$ diffractometer equipped with a modified LT-1 low-temperature apparatus. Unit cell parameters were obtained from a least-squares fit of 24 reflections with $36 \le 2\theta \le 50°$. No decay in the intensities of two standard reflections occurred. Data collection parameters are summarized in Table II.

$Au_3Cl_3(\mu$-dpma$)\cdot CH_2Cl_2$, 2. Colorless needle-like crystals were formed by slow evaporation of a dichloromethane solution of the complex. The unit cell parameters were obtained from a least-squares refinement of 10 reflections with $7° \le 2\theta \le 23°$. The space group $P2_1/n$ (no. 14) was uniquely determined by the observed conditions: $h0l$, $h + l = 2n$; $0k0$, $k = 2n$. Only random fluctuations (of less than 2%) in the intensities of two standard reflections were observed during the course of data collection. Data collection parameters are summarized in Table II. All other data collection procedures were identical with those of $Au_2Cl_2(\mu$-dpma).

$[Au_4Cl_4(\mu$-dpma$)_2](PF_6)_2\cdot 2CH_2Cl_2\cdot 2H_2O$, 3. Colorless prismatic crystals were formed by slow diffusion of diethyl ether into a dichloromethane solution of the compound. Unit cell parameters were obtained from a least-squares fit of 17 reflections with $6° \le 2\theta \le 27°$. The space group $P2_1/n$ was uniquely determined by the observed conditions: $h0l$, $h + l = 2n$; $0k0$, $k = 2n$. No decay in the intensities of two standard reflections occurred. Data collection parameters are summarized in Table II. All other data collection procedures were identical with those of $Au_2Cl_2(\mu$-dpma).

$[Au_4Cl_4(\mu$-dpma$)_2](NO_3)_2\cdot 4CH_3OH$, 4. Colorless prismatic crystals were formed by slow evaporation of the compound in a 1:1 mixture of CH_2Cl_2/CH_3OH. Unit cell parameters were obtained from a least-squares fit of 22 refections with $11° \le 2\theta \le 48°$. The space group $C2/c$ was determined by the observed conditions: hkl, $h + k = 2n$; $h0l$, $l = 2n$. No decay in the intensities of two standard reflections occurred. Data collection parameters are summarized in Table II. All other data collection procedures were identical with those of $Au_2Cl_2(\mu$-dpma).

Solution and Refinement of Structures. $Au_2Cl_2(\mu$-dpma$)\cdot 2.5C_6H_5CH_3$. All structure determination calculations were done on a Data General Eclipse MV/10000 computer using the SHELXTL Version 5 software package. The positions of the two gold atoms were generated from FMAP8, the Patterson-solving routine of SHELXTL. Other atom positions were located from successive difference Fourier maps. Phenyl rings were refined as rigid bodies. Anisotropic thermal parameters were assigned to the elements gold, arsenic, phosphorus, and chlorine. Isotropic thermal parameters were used for all other atoms. Distances were fixed about P(1), P(2), and As. The final stages of refinement included an absorption correction.[23] The final R value of 0.065 was computed with a data-to-parameter ratio of 31.8. This yields goodness-of-fit of 1.089 and a maximum shift/esd of −0.021 for U_{11} of C(49) in the last cycle of refinement. A value of 3 e/Å^3 was found as the largest feature on the final difference Fourier map. This peak was located 1.01 Å from a gold atom.

The weighting scheme used was $w = [\sigma^2(F_o)]^{-1}$. Scattering factors and corrections for anomalous dispersion were taken from a standard source.[24] Corrections for anomalous dispersion were applied to all atoms.

$Au_3Cl_3(\mu$-dpma)·CH_2Cl_2. The positions of the three gold atoms were determined from a sharpened Patterson map. Other atom positions were located from successive difference Fourier maps. Anisotropic thermal parameters were assigned to the elements gold, arsenic, chlorine, and phosphorus. Isotropic thermal parameters were used for all other atoms. All hydrogen atoms were fixed at calculated positions by using a riding model in which the C-H vector was fixed at 0.96 Å, and the isotropic thermal parameter for each hydrogen atom was given a value 20% greater than the carbon atom to which it is bonded. The final stages of refinement included an absorption correcton as described for $Au_2Cl_2(\mu$-dpma). The final R value of 0.051 was computed with a data-to-parameter ratio of 17.6. This yielded a goodness-of-fit of 0.925 and a maximum shift/esd of 0.008 for overall scale on the last cycle of refinement. A value of 2.12 e/Å^3 was found as the largest feature in the final difference Fourier map. This peak was located 1.17 Å from Au(2). The weighting scheme used was $w = [\sigma^2(F_o)]^{-1}$.

$[Au_4Cl_2(\mu$-dpma)$_2][PF_6]_2$·$2CH_2Cl_2$·$2H_2O$. The positions of Au(1) and Au(2) were generated from FMAP8. Other atom positions were located from successive difference Fourier maps. The other half of the molecule is generated by inversion. Anisotropic thermal parameters were assigned to the elements gold, arsenic, phosphorus, and chlorine. Anisotropic thermal parameters were also assigned to the phosphorus and fluorine on the anion, each chlorine atom on the dichloromethane solvent molecule, and the oxygen atom on the water molecule. Isotropic thermal parameters were used on all other atoms. The final stages of refinement included an absorption correction and the treatment of all hydrogen atoms as described. The final R value of 0.049 was computed with a data-to-parameter ratio of 14.1. This yielded a goodness-of-fit of 1.040 and a maximum shift/esd of 0.011 for Z/c at C(19) in the last cycle of refinement. A value of 1.79 e/Å^3 was found as the largest feature on the final difference Fourier map. This peak was located 1.15 Å from Au(2). The weighting scheme used was $w = [\sigma^2(F_o)]^{-1}$.

$[Au_4Cl_2(\mu$-dpma)$_2][NO_3]_2$·$4CH_3OH$. The positions of Au(1) and Au(2) were generated from FMAP8. Other atom positions were located from successive difference Fourier maps. Anisotropic thermal parameters were assigned to the elements gold, arsenic, phosphorus, and chlorine. Anisotropic thermal parameters were also assigned to the nitrogen and oxygen on the anion and each oxygen atom on the methanol solvent molecules. Isotropic thermal parameters were used on all other atoms. The final stages of refinement included an absorption correction and treatment of all hydrogen atoms as described for $Au_3Cl_3(\mu$-dpma). The final R value of 0.088 was computed with a data-to-parameter ratio of 16.9. This yielded a goodness-of-fit of 0.937 and a maximum shift/esd of 0.004 for y at C(30) on the last cycle of refinement. A value of 6.34 e/Å^3 was found as the largest feature on the final difference Fourier map. This peak was located 1.15 Å from Au(1).

Acknowledgment. We thank the National Science Foundation (CHE-8519557 and CHE-8941029) for financial support.

Supplementary Material Available: Tables of atomic coordinates, bond distances, bond angles, anisotropic thermal parameters, and hydrogen atom positions for $Au_2Cl_2(\mu$-dpma)·$2.5C_6H_5CH_3$, $Au_3Cl_3(\mu$-dpma)·CH_2Cl_2, $[Au_4Cl_2(\mu$-dpma$)_2][PF_6]_2$·$2CH_2Cl_2$·$2H_2O$, and $[Au_4Cl_2(\mu$-dpma$)_2][NO_3]_2$·$4CH_3OH$ (18 pages); listings of observed and calculated structure factors (103 pages). Ordering information is given on any current masthead page.

(24) The method obtains an empirical absorption tensor from an expression relating F_o and F_c. Moezzi, B., Ph.D. Thesis, University of California, Davis, 1987.

(25) *International Tables for X-ray Crystallography*; Kynoch Press: Birmingham, England, 1974; Vol. 4.

Mechanism of Reduction of Trityl Halides by Lithium Dialkylamide Bases

Martin Newcomb,* Thomas R. Varick, and Swee-Hock Goh[1]

Contribution from the Department of Chemistry, Texas A&M University, College Station, Texas 77843. *Received November 2, 1989*

Abstract: Trityl chloride (TCl) and bromide are reduced by hindered lithium dialkylamide bases in THF to give predominantly triphenylmethane and a small amount of trityl dimer. Rate constants for the reduction of TCl by lithium diisopropylamide and lithium *tert*-butylethylamide in THF at −78 °C have been measured; the reactions are first order in monomeric base and in trityl chloride. Inter- and intramolecular kinetic isotope effect studies employing β-deuterium substituted bases and substituent effect studies coupled with other kinetic information were used to formulate a scheme for the reactions. The reactions proceed by a rapid predissociation of the trityl halide to form an ion pair containing the trityl–THF oxonium cation followed by diffusion controlled electron transfer (ET) from the monomeric form of the base to the trityl–THF oxonium ion. The radical pair thus formed reacts by fast, highly regioselective β-hydrogen atom transfer from the aminyl radical to the methine carbon of the trityl radical to give triphenylmethane. Radical escape from the cage is a minor competing process. An outer-sphere ET process is energetically acceptable, but an inner-sphere process appears to be more likely.

For several years, our group has been interested in the possibility that hindered lithium dialkylamide bases could react with weak organic oxidants by an electron transfer (ET) process rather than a more conventional heterolytic deprotonation. Several reports appearing since the late 1970s provided evidence that ET reactions from lithium dialkylamides (especially LDA) to a variety of organic substrates might occur.[2] Generally, these studies were product oriented, and, for those that reached mechanistic conclusions, the mechanisms typically were inferred from the detection of radical or radical anion species (or the products derived therefrom) formed from the organic substrate. Our efforts have involved kinetic studies and the application of lithium dialkylamide probes that were designed to signal an ET process by providing upon oxidation aminyl radicals that would rearrange.[3,4] The culmination of the probe work resulted in the observation that electron transfer from $LiNR_2$ was only apparent when the re-

(1) Department of Chemistry, University of Malaya, 59100 Kuala Lumpur, Malaysia.

(2) For leading references, see: Scott, L. T.; Carlin, K. J.; Schultz, T. H. *Tetrahedron Lett.* **1978**, 4637. Ashby, E. C.; Goel, A. B.; DePriest, R. N. *Ibid.* **1981**, *22*, 4355. De Kimpe, N.; Yao, Z.; Schamp, N. *Ibid.* **1986**, *27*, 1707. Williams, R. M.; Armstrong, R. W.; Dung, J.-S. *J. Am. Chem. Soc.* **1985**, *107*, 3253. Newkome, G. R.; Hager, D. C. *J. Org. Chem.* **1982**, *47*, 599. A more complete list of references is given in ref 3.

(3) Newcomb, M.; Burchill, M. T.; Deeb, T. M. *J. Am. Chem. Soc.* **1988**, *110*, 6528.

(4) Newcomb, M.; Burchill, M. T. *J. Am. Chem. Soc.* **1983**, *105*, 7759. Newcomb, M.; Burchill, M. T. *J. Am. Chem. Soc.* **1984**, *106*, 2450, 8276. Newcomb, M.; Williams, W. G. *Tetrahedron Lett.* **1984**, *25*, 2723.

0002-7863/90/1512-5186$02.50/0